



**282746  
IMPACT2C**

**Quantifying projected impacts under 2°C warming**

Instrument Large-scale Integrating Project  
Thematic Priority FP7-ENV.2011.1.1.6-1

**D2.1: Identification of robust climate change patterns in pre-existing scenarios for Europe**

Due date of deliverable 30.09.2012  
Actual submission date  
Start date of the project 01.10.2011  
Duration 48 months  
Organisation name of lead contractor for this deliverable CNRS – IPSL

Revision: V2.0

Project co-funded by the European Commission within the Seventh Framework Programme		
Dissemination Level		
<b>PU</b>	Public	X
<b>PP</b>	Restricted to other programme participants (including the Commission Services)	
<b>RE</b>	Restricted to a group specified by the consortium (including the Commission Services)	
<b>CO</b>	Confidential, only for members of the consortium (including the Commission Services)	

## Authors

Robert Vautard (CNRS-IPSL), Andreas Gobiet (UNIGRAZ), Erik Kjellström (SMHI), Grigory Nikulin (SMHI), Stefan Sobolowski (Uni-Res), Annemiek Stegehuis (CNRS-IPSL), Pascal Yiou (CNRS-IPSL)

## Objectives

In accordance with the IMPACT2C DoW of Task 2.1, an analysis aiming at identifying robust patterns of climate change in existing scenarios for Europe has been conducted. This study calculated changes in future European climate under the socio-economic emission scenario A1B (Nakicenovic et al., 2000) as simulated from global models of the ENSEMBLES project (Hewitt & Griggs 2004), and downscaled by regional climate models (RCMs). One of the aims is to estimate the changes in classical variables (temperature, precipitation, wind, sea level pressure,...) and less classical, but explanatory variables related to the surface energy budget (heat fluxes) in order to assess expected changes in the European climate and their uncertainties for a global temperature change of +2°C and +1.5°C compared to preindustrial times. For a given socio-economic scenario, model projections usually differ due to several factors: internal variability of climate, global model sensitivity to changes in radiative forcing, and regional patterns of change. The focus on comparing climates over fixed global temperature change periods with a control current climate reduces the uncertainty due to climate model sensitivity. Thus, for a fixed global temperature change, the differences between two projections should be dominated by the way the full chain of models (global and regional) represents the regional climate over Europe, once internal variability has been smoothed out. The robust patterns of changes can be estimated as the patterns that appear in most of such model projections.

The study is actually twofold:

- The first objective is to describe regional climate changes in Europe assuming +2°C and +1.5°C global warming and their uncertainties.
- The second objective is to estimate the part of the uncertainty that is removed due to considering periods defined by global warming instead of time.

We focus on main variables such as temperature, precipitation, sea level pressure and winds, changes in their average and extremes, and on less classical but more explanatory variables such as surface fluxes.

## Methodology

We identified the robust changes by calculating ensemble averages and standard deviations of RCM simulations corresponding to time periods of global temperature changes identified in driving GCMs (see Table 1 below). We used scenario A1B simulations of the ENSEMBLES project and analysed them in “global temperature periods”, based on the analysis of time periods when global mean temperature (30 year sliding average) reaches +2°C or +1.5°C, respectively, compared to pre-industrial times (see SubDeliverable 2.1.1 for exact definition of the +2°C period). These global temperature periods were compared to the reference period 1971 – 2000 to derive climate change signals. In addition, a fixed-time period (2031-2060, centred at 2045) was selected in order to compare the spread of the climate change signals based on the global temperature controlled and the time controlled periods(+2°C – control and 2045 – control). For each of the model projections, we calculated averages of several variables and calculated the difference with the reference periods. Due to the definition of the +2°C period relative to pre-industrial, the global temperature difference between the +2°C period and the reference period is actually 1.54°C for each GCM, and +1.04°C for the +1.5°C period.

We used bias-adjusted data (from WP4) whenever available, i.e. for temperature and precipitation. Bias adjustment is based on a quantile mapping approach, as described by Themeßl et al. [2011; 2012], and the E-Obs version 5 gridded dataset (Haylock et al. 2008).

GCM	RCM	+2°C central year	+2°C period	+1.5°C central year	+1.5°C period
bccr_bcm2_0-r1	RCA	2052	2038 – 2067	2039	2025 – 2053
	HIRHAM				
HadCM3Q0	RCA	2035	2021 – 2050	2022	2008 – 2037
	CLM				
	HadRM				
HadCM3Q16	HadRM	2028	2014 – 2043	2016	2002 – 2031
HadCM3Q3	RCA	2047	2033 – 2062	2028	2014 – 2043
	HadRM				
mpi_echam5-r3	RegCM	2048	2034 – 2063	2035	2021 – 2050
	REMO				
	HIRHAM				
	RACMO				
	RCA				
ARPEGE	ALADIN	2043	2029 – 2058	2028	2014 – 2043
	HIRHAM				

Table 1: Time period for which +2°C and +1.5°C compared to pre-industrial times was reached in ENSEMBLES A1B global climate projections

The robust patterns of changes are calculated as ensemble averages over the 15 RCM-GCM pairs (the entire available set of simulations from ENSEMBLES reaching beyond 2050), and the number of RCMs that agree on the sign of the change, as well as the ensemble standard deviation are used to characterize robustness. The uncertainty due to GCM sensitivity is estimated from changes in the ensemble standard deviation between temperature-controlled and time-controlled periods.

### Temperature changes

Figure 1 shows the mean temperature as simulated by the RCMs over the control period and changes in °K between the +2°C period and the control period, in Winter and Summer, together with the ensemble standard deviation of the changes. Average changes have the same pattern as those described for fixed time periods in several regional ensemble simulations (Fischer and Schär, 2010; Kjellström et al., 2011): an increase of temperature is found everywhere for all models, with enhancement in North-eastern and Eastern parts of Europe in winter (2-3°C) and in Southern Europe in summer (2-3°C). The regional warming exceeds the global warming in most areas but the British Isles and Iceland, where the influence of the moderate warming of the North Atlantic is seen in all seasons. In summer a relatively small warming is also seen close to the North Sea and the Baltic Sea. The ensemble standard deviation of the changes remains much smaller than the amplitude of changes (about 3-10 times smaller) everywhere.

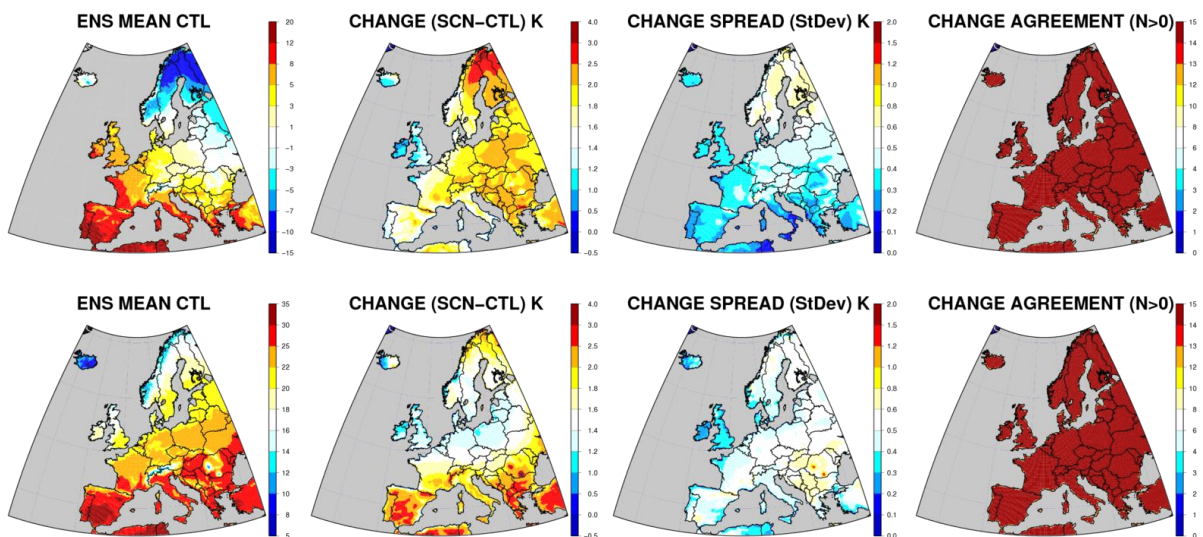


Figure 1: (left panels) Average RCM simulated temperature (°C) during the control period (1971 – 2000); (middle left panels): ensemble average of changes between control and +2°C period. The white color stands for the interval 1.4 – 1.6°C, which corresponds to the global temperature difference in each simulation between the +2°C period and the control period. (middle right panels) Standard deviation of the climate change signal. (right panels) Number of models agreeing on an increase in temperature. Results are shown for winter (upper panels) and summer (lower panels).

For a +1.5°C change the patterns are similar but of smaller amplitudes (see Figure 2). Regional changes are fairly linear as a function of global temperature as their amplitude is about 2/3 of changes in the +2°C case (Figure 3). This ratio is expected due to the definition of the +2°C and +1.5°C periods, since the global warming since the reference period is respectively 1.54°C and 1.04°C (see above), leading to a ratio of  $1.04/1.54=0.68$ . The scalability of the changes is high in both seasons since the correlations between changes taken at each land grid point (the correlation of the two clouds of points in Figure 3) are respectively 0.99 in winter and 0.98 in summer.

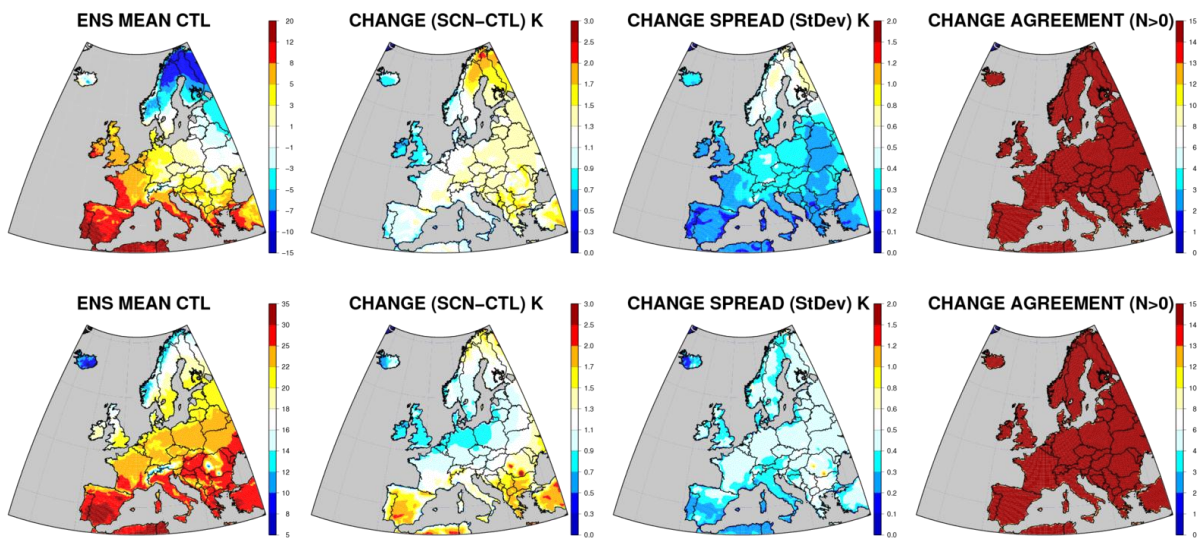


Figure 2: Same as in Figure 1 for +1.5°C global temperature change (Top=Winter; Bottom=Summer, left=absolute values in reference period, middle left=changes between the two periods, middle right=ensemble standard deviation of changes, right=number of models with positive change).

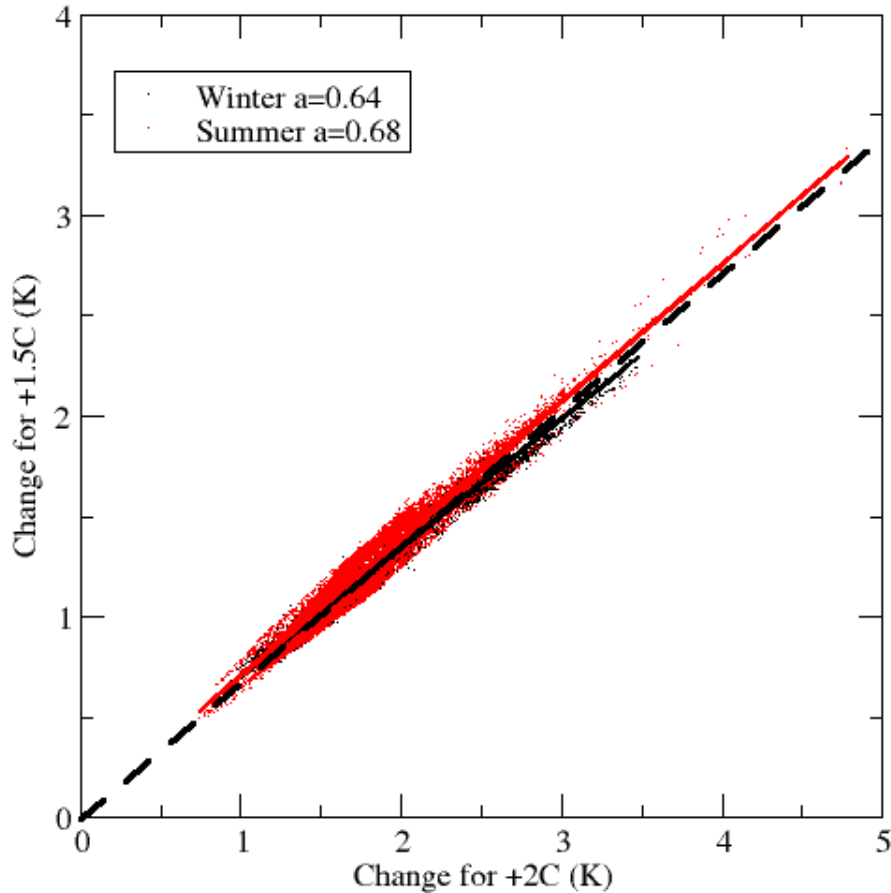


Figure 3: Scatter plot of changes in Europe between the 1971-2000 period and the +1.5°C period vs. changes obtained for +2°C. Each point in the plot corresponds to a land grid point. The dashed line stands for the “expected” ratio relation between changes obtained if the +1.5°C case perfectly scaled with the +2°C case, with a 0.68 slope. The “a” coefficient is the regression slope effectively calculated (black=winter, red=summer).

Extreme temperature changes are given as changes in 20-year return values. These are calculated using extreme value analysis where the estimated probabilities of extreme events are expressed in terms of 20-year return values. The 20-year return value can be looked upon as the threshold that is exceeded once every 20 years and 20 years is then referred to as the return period. The procedure used for calculating the return values is described in detail in Nikulin et al. (2011). Here we present results for changes in 20-year return values in daily maximum and daily minimum temperatures. For daily maximum temperatures (Figure 4), the largest changes (3-4°C) are found over Central and Eastern Europe in winter and over South-Eastern Europe and the Iberian Peninsula in summer. In areas where this value is highest (Iberian Peninsula, France, the Balkans) the 20-year return value is expected to rise well above 40°C. The spread between the models is generally highest in the Central and Eastern Europe in summer. In parts of this area, notably Finland, there are even models indicating no increase in extreme maximum temperatures. Discrepancies in this area may to some extent be related to how different RCMs treat lakes as parts of this area has a large fraction of lakes

that have an impact on the regional climate (Samuelsson et al., 2010). Low extremes of daily minimum temperature extremes (Figure 5) undergo a larger change in winter, ranging from 2-3°C degrees in central and Southern Europe to 5-8°C in Scandinavia and Russia. In summer the 20-year daily minimum temperature extreme change is more homogeneous (about 1-2°C). Note the large spread in model responses in winter over Central Europe, where the models do not agree on the sign of the change in extreme temperatures and several models even exhibit cooling of the extremes.

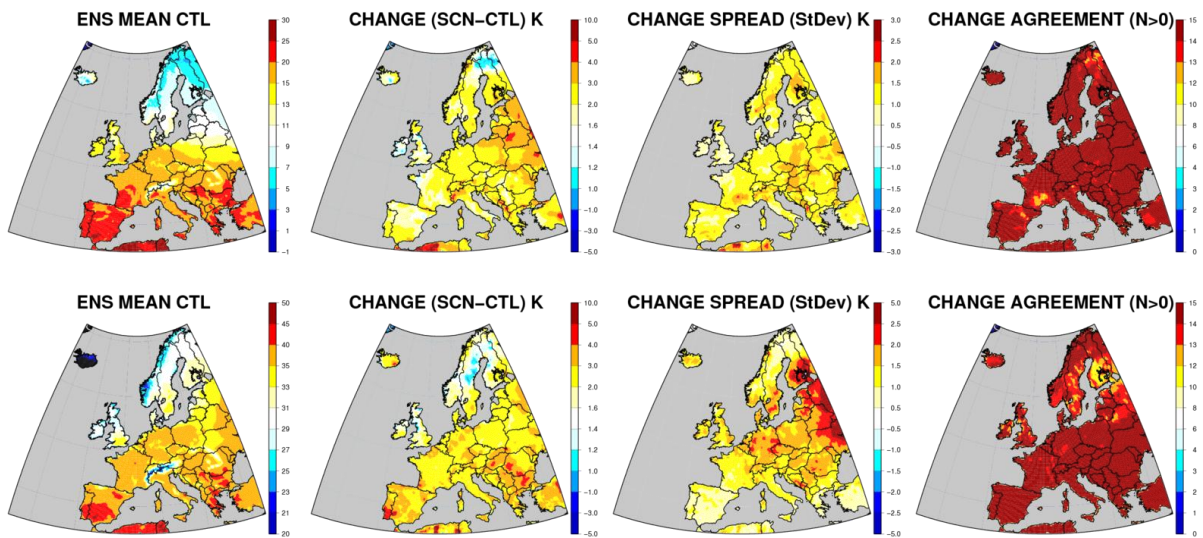


Figure 4 : Same as Figure 1 (Top=Winter; Bottom=Summer, left=absolute values in reference period, middle left=changes between the two periods, middle right=ensemble standard deviation of changes, right=number of models with positive change) for the Tmax 20-year return value.

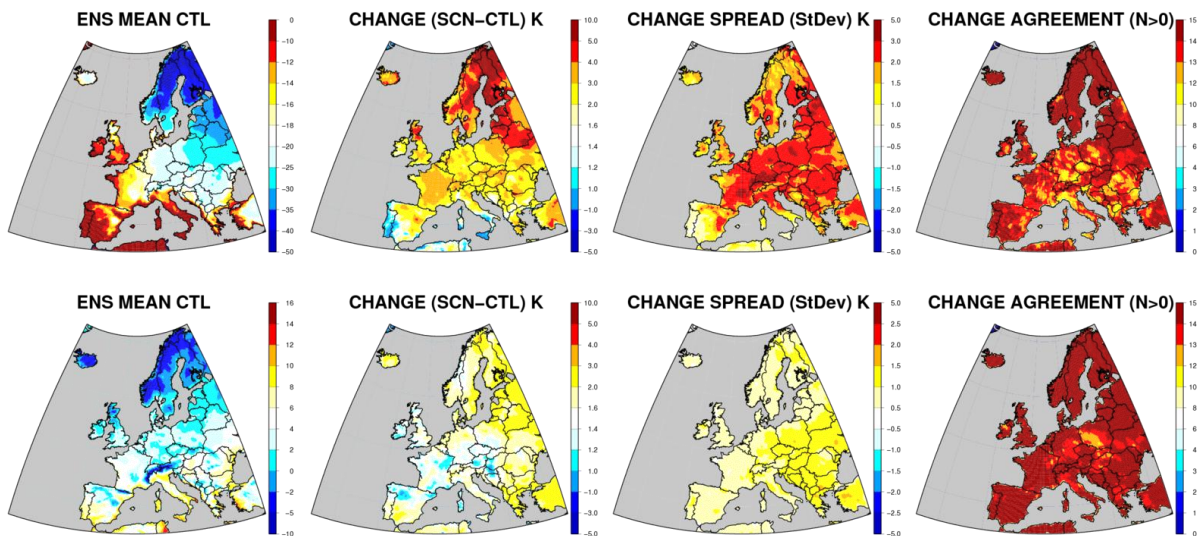


Figure 5 : Same as Figure 4 for the low Tmin 20-year return value.

Changes obtained for the +1.5°C case in general scale well with the +2°C change, with local amplitude changes about 2/3 of the +2°C change (see Figure 6), but this scalability is less pronounced that for mean temperatures. For some regions a nonlinear behaviour appears (not shown). For instance, for Tmax over Scandinavia in summer, the change appears to “saturate”, with values for +2°C close to those for +1.5°C. By contrast amplification can be found for Tmin in winter, when changes at +2°C are higher than when scaled with changes at +1.5°C. The right part of the cloud of points in Figure 6 (right) contains points over North-Eastern Europe and Scandinavia, where amplification could be due to snow albedo feed-back. We also note that the degree of correlation is considerably lower compared to when we look at the seasonal means (Figure 3) indicative of the larger uncertainty associated with the extreme value statistics.

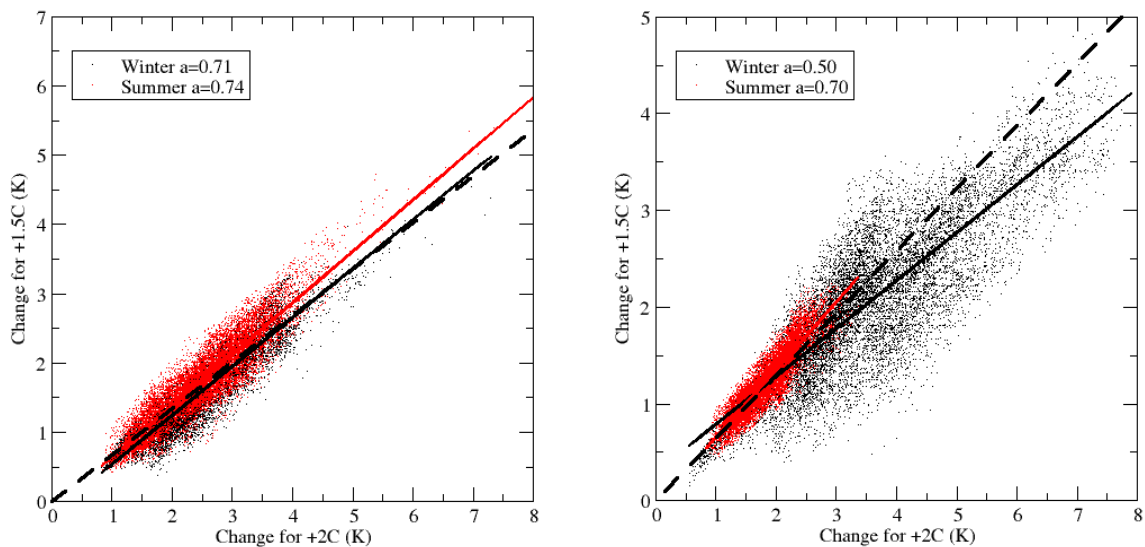


Figure 6: Scatter plot of grid point Tmax (left, in K) and Tmin (right, in K), for changes 1.5°C-CTL vs. 2°C-CTL. Red dots stand for Summer and black dots for Winter. The dashed line stands for the “expected” ratio relation between changes obtained if the +1.5°C case perfectly scaled with the +2°C case.

### Precipitation changes

Precipitation amount patterns are also well defined. In winter a general increase is found with maximum values in Northern Europe, especially along the coast of the North Sea and the Baltic Sea, where all models agree upon more precipitation (Figure 7). The increase reaches 10-15%. In Southern Europe models do not agree on sign except over a few areas (Southern Italy, Greece). In summer, significant decrease of precipitation of also about 10-15% is found in South-Central Europe, with a general model agreement, together with an increase in precipitation over Scandinavia. The only area where all models agree on the sign of change is Scandinavia (increase in both seasons) and in

summer some smaller areas in south-eastern Europe and the west coasts of Spain, France and the southern British Island (decrease in summer).

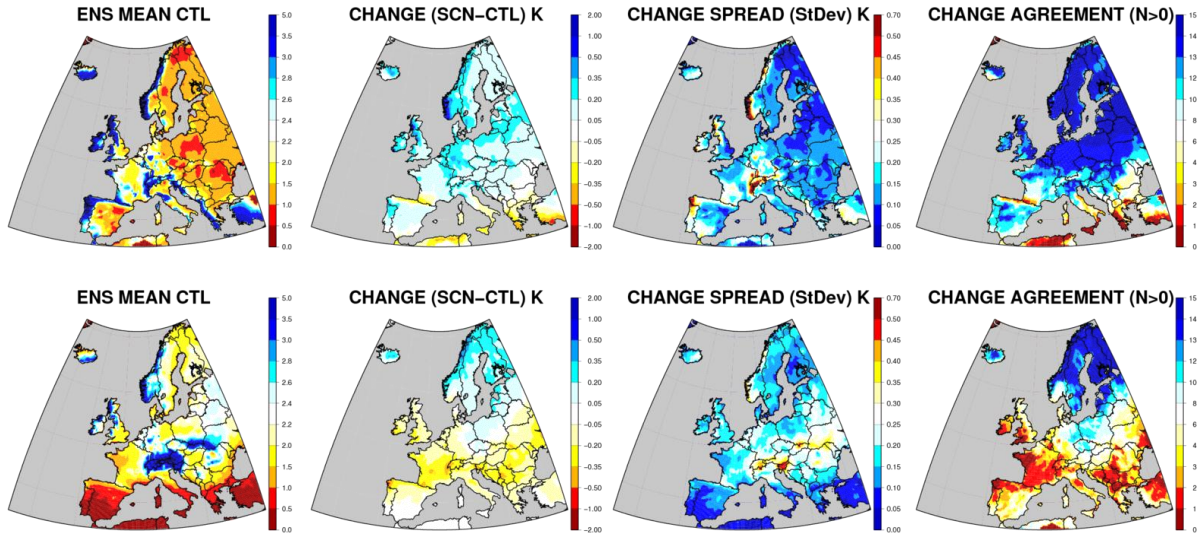


Figure 7: Changes obtained with a global warming of +2°C for daily precipitation amount, as in Figure 1 (Top=Winter; Bottom=Summer, left=absolute values in reference period, middle left=changes between the two periods, middle right=ensemble standard deviation of changes, right=number of models with positive change).

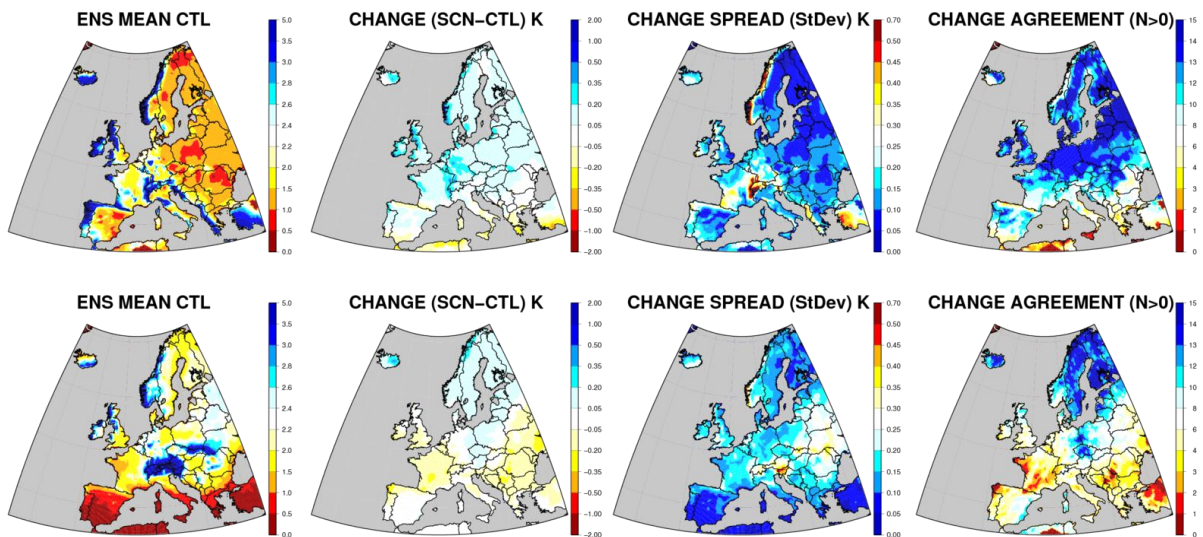


Figure 8: As in Figure 7 for changes associated to a +1.5°C global warming

For a +1.5°C change the same patterns are found with smaller amplitude (Figure 8), with a fairly linear scaling (spatial correlation of changes over land of  $r=0.92$  in winter and  $r=0.95$  in summer). The robustness, as depicted by model agreement, is less pronounced than for the +2°C global change. Changes in extremes of heavy precipitation defined as the 20-year return value calculated from extreme value theory in the same way as outlined for temperature above are shown in Figure 9. The

ensemble mean exhibit positive changes in all areas both in summer and winter (Figure 9), with an amplitude ranging from 5% to about 15%. The increase is marked over Eastern Europe and Scandinavia in summer and over Southern Europe in winter. This increase is found in a majority of models in most areas, but not all. Uncertainties remain large in the southernmost areas of Europe. Compared to the changes in seasonal means the changes in extremes are less spatially coherent and individual models exhibit patchy structures (see Figure 10 as an example). Note that in some models scattered areas of decrease in 20-year return values are even found, without inter-model agreement on locations.

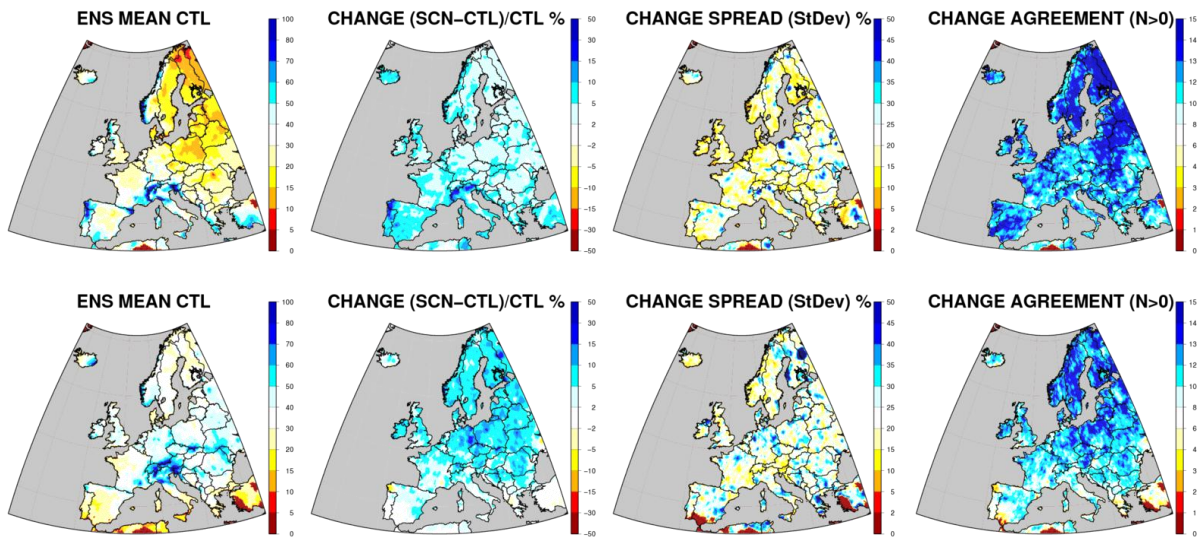


Figure 9: As in Figure 4 for precipitation 20-year return value (Top=Winter; Bottom=Summer, left=absolute values in reference period, middle left=changes between the two periods, middle right=ensemble standard deviation of changes, right=number of models with positive change).

20-yr ret. values of Precipitation (pr) | bias-corr | JJA | CTL: 1971-2000 | SCN: 2°C warming

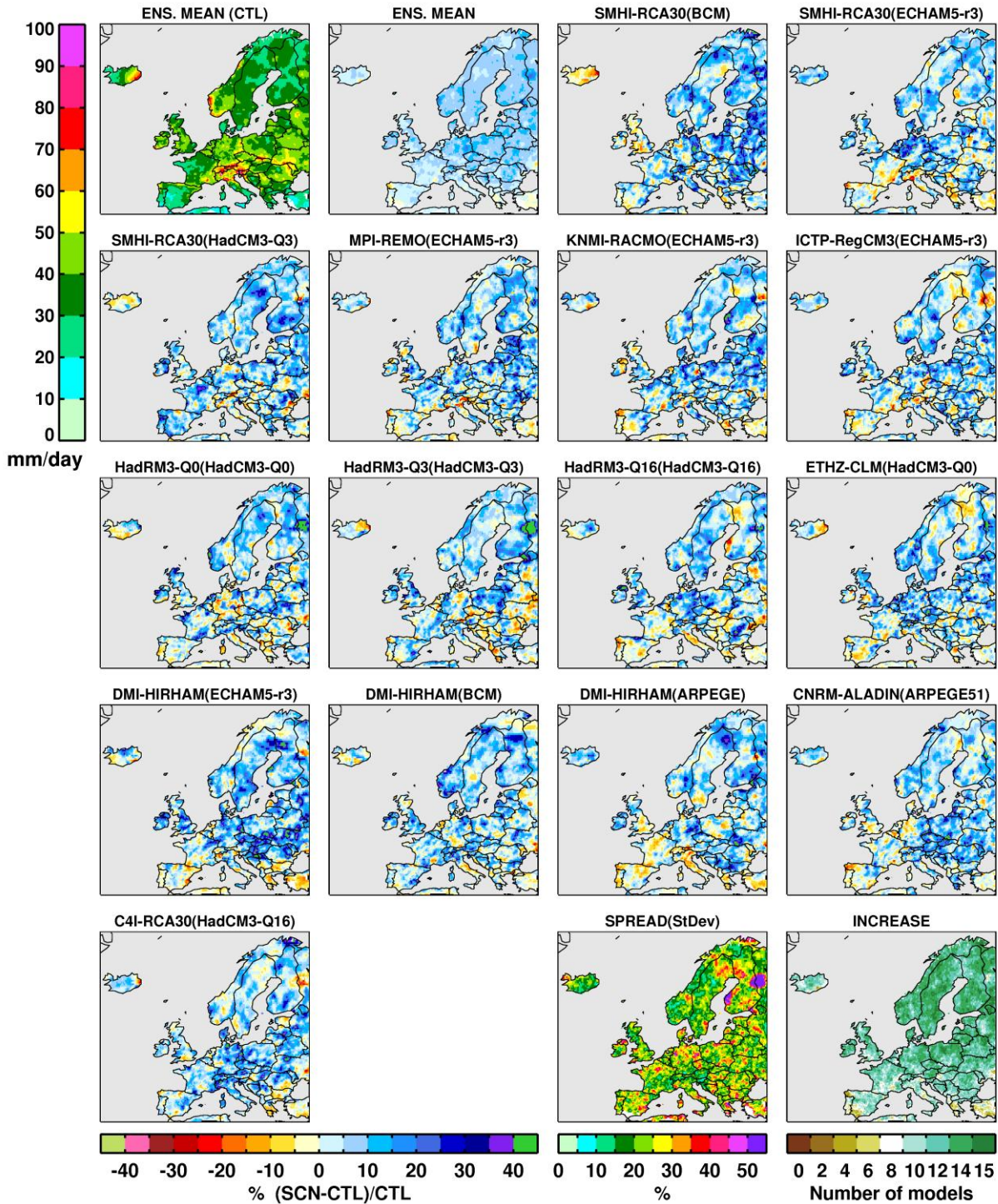


Figure 10: summer changes of extreme precipitation 20-year return value (in mm/Day) ensemble mean (top left), mean change (second top left) under the +2°C global warming, changes in 20-year return values in individual models. The two bottom right panels show the ensemble standard deviation and the change agreement as in Figure 9.

### Extreme wind changes

Windstorms are among the most damaging extreme events. Extreme winds are calculated here as the 99<sup>th</sup> percentile of the daily maximum 10-meter wind speed for each season (I99). For reference, we present a few values from the Beaufort wind scale, which defines a number of wind speed ranges and associated expected damages to the environment and human infrastructure. Wind speeds of ~15, 19 and 23 m/s are associated with near gale, gale and severe gale force winds, respectively. It is above 23 m/s that damage to life and property is seen to increase substantially (e.g. dangerous surf, uprooted trees, roof and building damages).

Figure 11 shows the ensemble mean I99 winds as simulated by the RCMs over the control period and changes (in %) between the +2°C period and the control period, in Winter and Summer, together with the ensemble standard deviation of changes and model agreement (an indication of robustness). Relatively robust increases of extreme winds (more than 12 models out of 15 agree in sign) of up to 10% are seen over some areas of Central/Eastern Europe in winter. Over other regions the change is generally positive but modest and generally not robust with substantial model disagreement on the sign of the change. In summer relatively robust increases (decreases) are seen over Scandinavia (Western Europe) (figure 11, bottom row). The spread of the changes is spatially and seasonally quite variable with some regions indicating spreads which are larger than the simulated changes in one season and not in the other (e.g. Norway).

In the +1.5C time period the patterns and magnitudes of the I99 wind changes are generally similar to the +2C time period for both seasons (Figure 12). There are some subtle differences, however. For example, in winter the increases are *more* robust and of *greater* magnitude across Western Europe in the +1.5C case (compare top rows of figures 11, 12). Conversely, the summer decrease in I99 winds across Western Europe is *less* robust and *weaker* during the +1.5C time period (compare bottom rows of figures 11, 12). The spread of the changes exhibits characteristics during the +1.5C period that are similar, both spatially and temporally, to the +2C period.

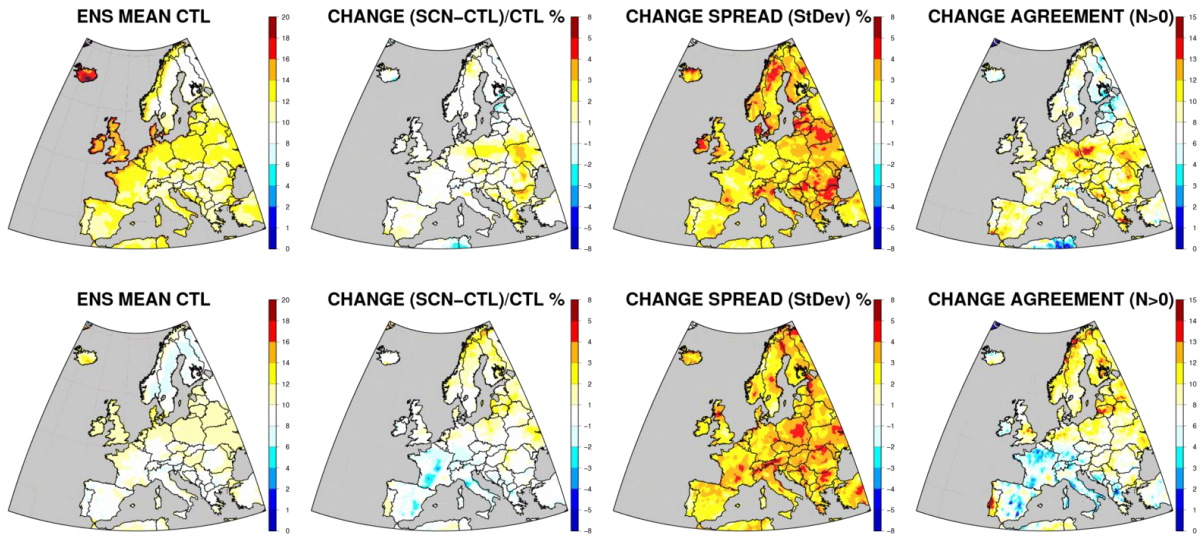


Figure 11: Changes in I99 winds for the time periods corresponding to +2C global warming. Units are m/s for CTL, change and spread are shown as percentages (Top=Winter; Bottom=Summer, left=absolute values in reference period, middle left=changes between the two periods, middle right=ensemble standard deviation of changes, right=number of models with positive change).

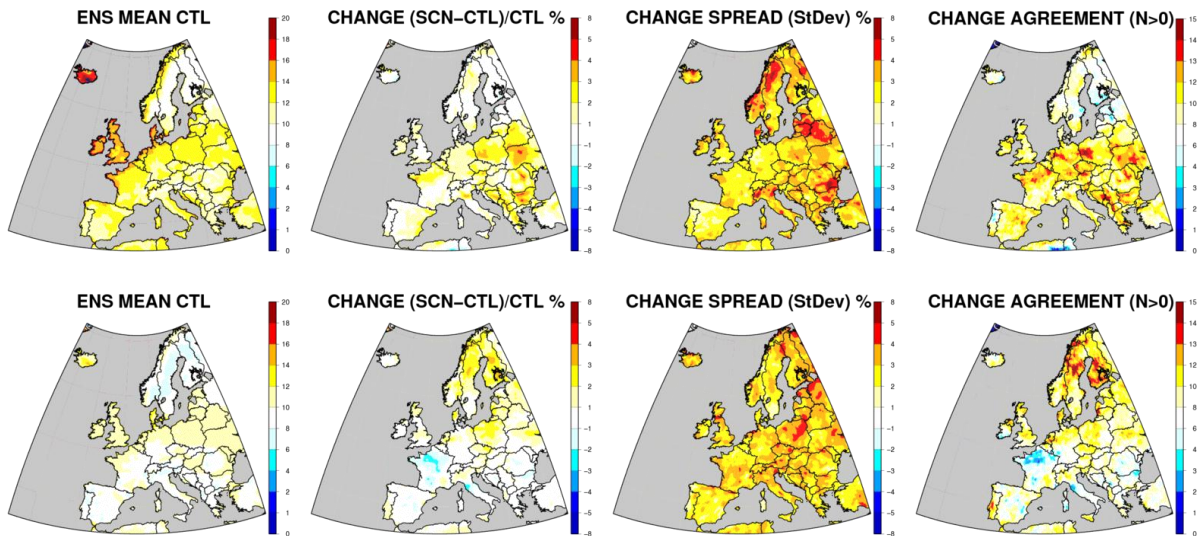


Figure 12: Same as Figure 11, but for time periods corresponding to +1.5C global warming. Units are m/s for CTL, change and spread are shown as percentages.

### Sea-level Pressure changes

Figure 13 shows the ensemble mean Sea Level Pressure (SLP) as simulated by the RCMs over the control period and changes (in hPa) between the +2°C period and the control period, in winter and summer, together with the ensemble standard deviation of changes and model agreement. The typical North-South climate change signal is visible and robust in the winter season with lower (higher) pressure in the north (south). The summer signal is also robust with most of the models

agreeing on modest decreases in SLP across southern Europe. The spread of the change in both seasons tends to be largest where model agreement is low and magnitude of the change is near zero. The patterns of SLP changes during the +1.5C period are virtually identical to the +2C period but the magnitudes are reduced as one might expect given the other surface change differences between the two periods (Figure 14). There is one obvious difference between the two periods, which is the spread of the SLP change. The spread of the changes in SLP in both seasons is generally larger during the +2C period than the +1.5C period.

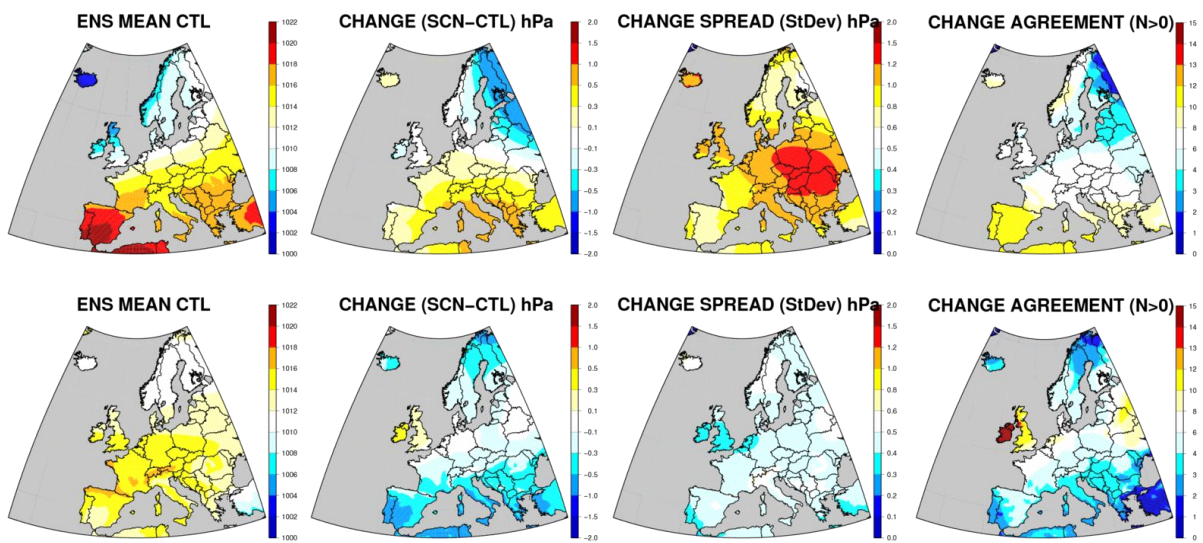


Figure 13: Changes in Sea Level Pressure for the time periods corresponding to +2C global warming. Units are hPa (Top=Winter; Bottom=Summer, left=absolute values in reference period, middle left=changes between the two periods, middle right=ensemble standard deviation of changes, right=number of models with positive change).

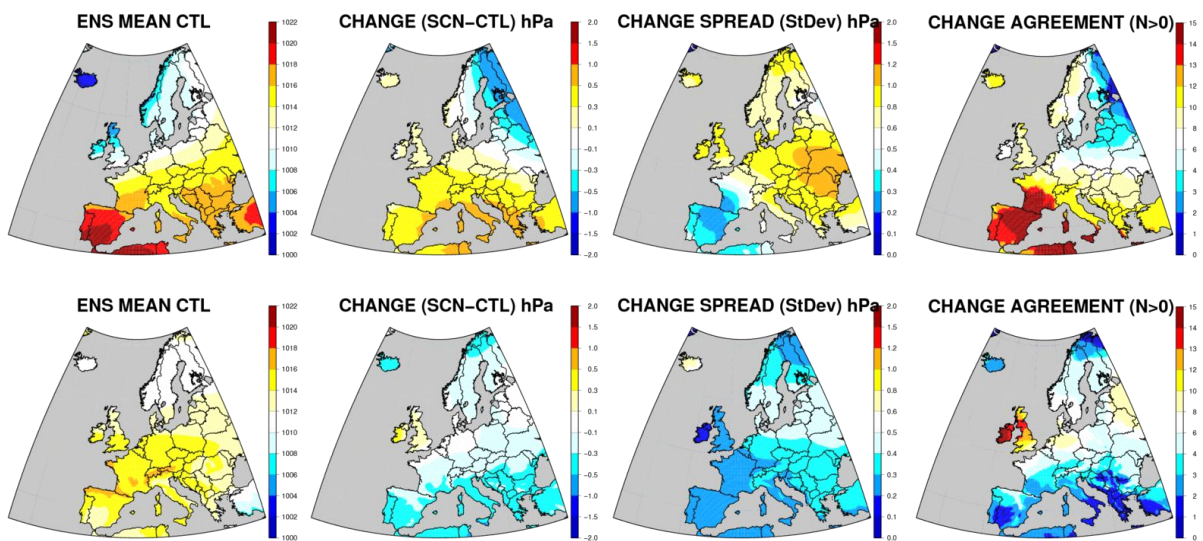


Figure 14: Same as figure 12, but for time periods corresponding to +1.5C global warming. Units are hPa.

## Surface fluxes

Surface weather changes are influenced both by dynamical changes and by changes in the physics of the vertical column above the surface. These latter changes are due to clouds, atmospheric composition, turbulence, soil moisture and temperature as well as land use properties. All these processes influence the surface energy budget, characterized by radiative and heat fluxes. We will consider here net short and long wave fluxes, sensible and latent upward fluxes. Since these changes have a more explanatory character than practical use for impacts and adaptation, we only consider here changes for +2°C periods for limiting the number of figures. Since fluxes are particularly important during the growing season and for land-atmosphere feedbacks, we consider here only spring (MAM) and summer (JJA) fluxes.

Spatial patterns of latent and sensible heat flux changes are shown in Figures 15 and 16. In spring, almost all models agree on an increase of latent heat except in southernmost areas and in other smaller areas such as North-Western coastal areas (this is also the case in fall and winter). This distribution is consistent with the energy-limited nature of evapotranspiration in Europe in spring (Teuling et al., 2008). In summer the latent heat increase is restricted to Northern areas while Southern areas, including large parts of Central Europe, have decreasing latent heat due to drought increase and soil moisture limitation. This drying causes an increase in sensible heat in summer in this area, with large model agreement, while over Scandinavia sensible heat fluxes decrease due to a wetter and cloudier climate. In spring, sensible heat flux only increase with high model agreement in southernmost areas. However fluxes are suspected to be biased on ensemble average in the ENSEMBLES simulations (Stegehuis et al., 2012; Fischer et al., 2012), with the effect of overestimating the ensemble mean changes and underestimating the inter-annual variability changes. It can also lead to a bias in temperature change although its sign is not obvious to deduce in the absence of further observational constraints.

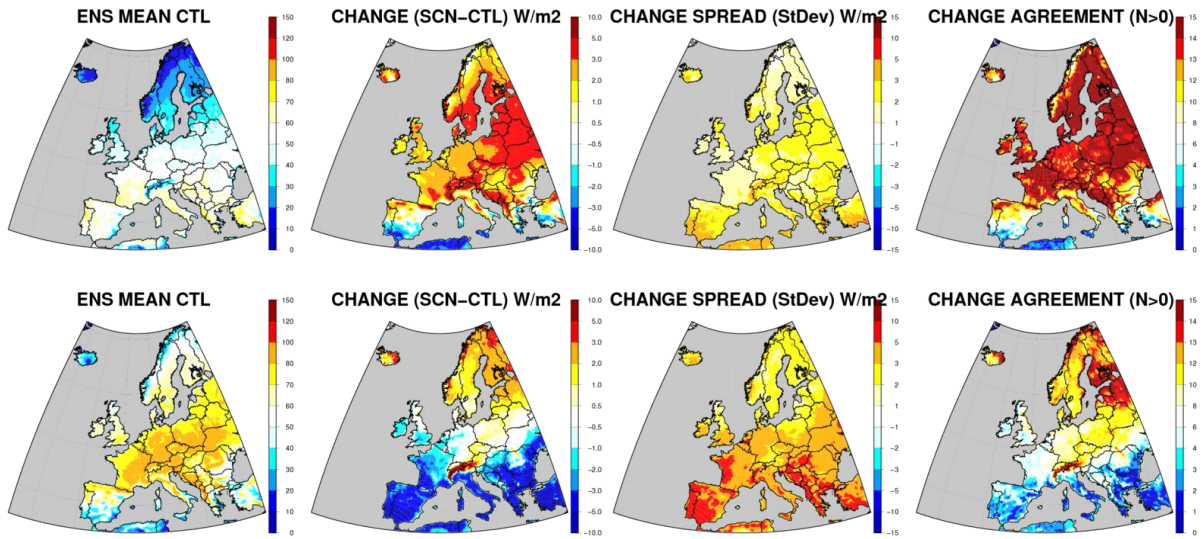


Figure 15 : As in Figure 1 for latent heat flux, but top panels stand for the spring season and bottom panels stand for the summer season (left=absolute values in reference period, middle left=changes between the two periods, middle right=ensemble standard deviation of changes, right=number of models with positive change)

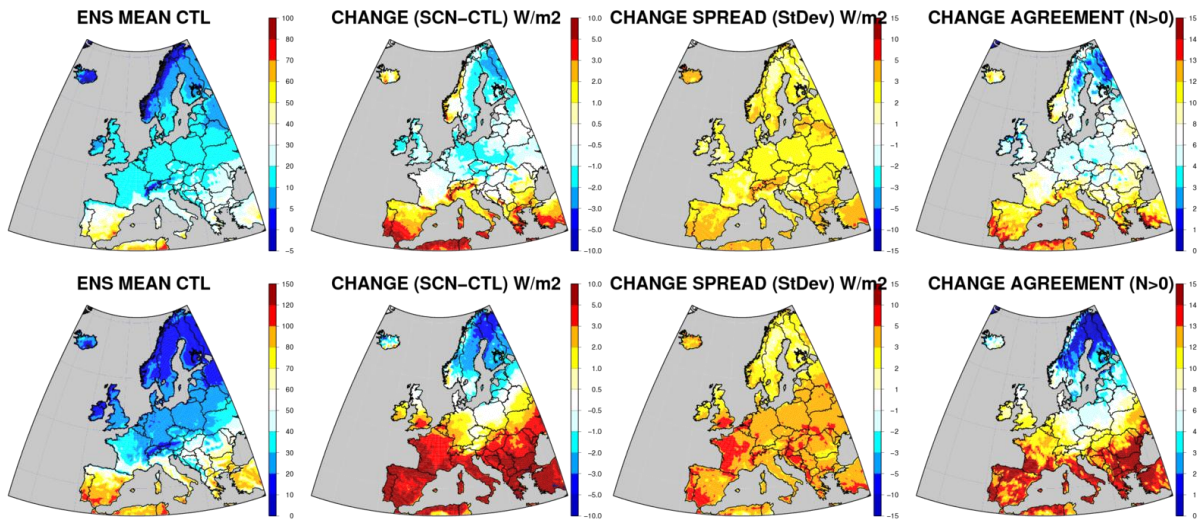


Figure 16 : As in Figure 14 for Sensible heat fluxes.

These heat flux changes respond to the changes in net radiative fluxes (Figure 17 and 18). In the two seasons, a robust increase in short-wave radiation is found in Southern Europe and robust increase in long-wave radiation is found in Northern Europe. In summer, the shortwave radiation increase extends Northward over central Europe where drying, increase of sensible heat and temperature also occurs. This extension is consistent with the northward propagation of drought and heat in the spring-summer transition described in Zampieri et al. (2009). It is noteworthy that sea-level pressure, however, does not exhibit an associated robust increase in anticyclonic weather over Mediterranean

areas in summer, which could be due to compensation due to heat surface pressure low. In Northern Europe, a wetter and cloudier weather induces an increase in long-wave radiation.

In fact, in summer there is compensation between the two flux changes in Northern Europe while in South-Central areas the shortwave radiation energy increase exceeds in amplitude the decrease in long-wave radiation. This energy excess is also found in the sum of heat flux changes (not shown). Thus, on average, there is a robust increase of incoming energy over South-Central Europe which induces a robust increase in sensible heat, consistent with the additional warming in these areas.

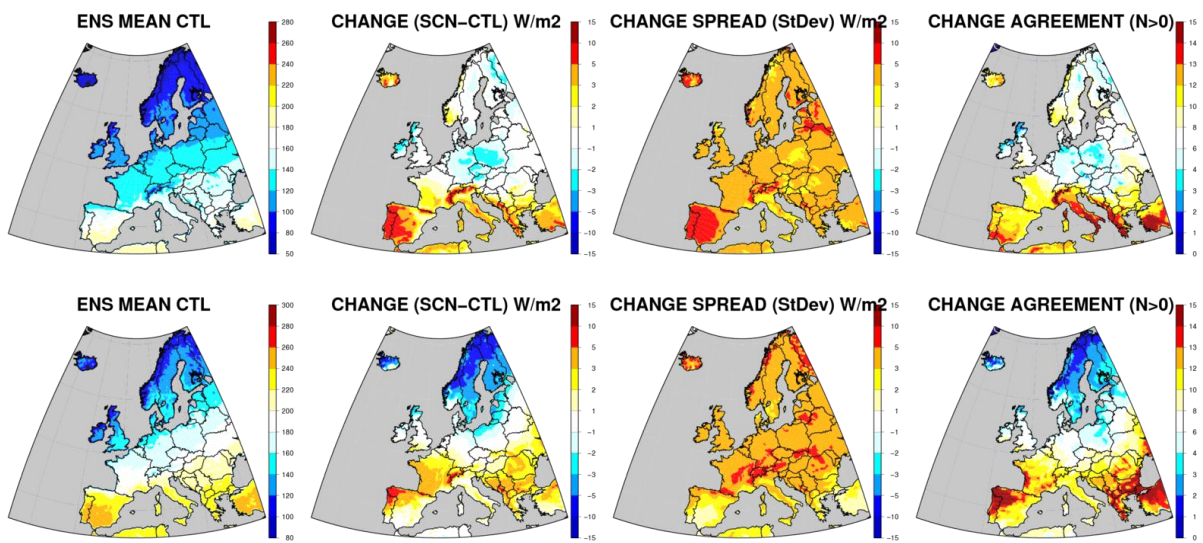


Figure 17: Same as in Figure 15 for net short-wave radiative fluxes

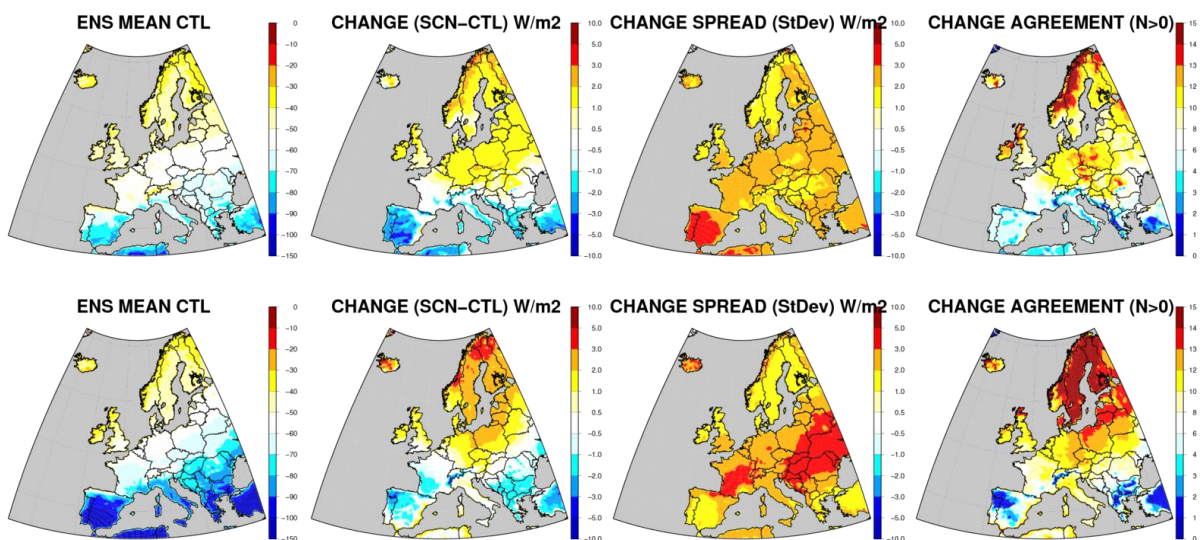


Figure 18: Same as in Figure 15 for net long-wave radiative fluxes

### Uncertainty of the +2°C changes vs. those of a fixed time period

Uncertainty in future climate is due to natural variability, emission scenario uncertainty, the uncertainty of model sensitivity to atmospheric composition changes, and other uncertainties related to climate models. We hypothesize that the spread of the change, or uncertainty, in a variable of interest should decrease when one selects periods based on a temperature (e.g. +2C) rather than a temporal threshold (e.g. mid-century), as this removes the uncertainty on global model sensitivity. In this study a future period roughly corresponding to the average time at which the driving GCMs cross the +2C threshold is chosen (2031-2060) to evaluate the claim that climate change investigations based around temperature periods reduces uncertainty. The reduction in spread is expected to be most visible in variables closely linked to the global warming signal. Noisy, synoptic fields related to weather noise are less likely to show a coherent reduction in uncertainty.

For instance, changes in regional temperature have less uncertainty in the +2°C scenario than in the fixed time period case in all seasons, as seen on the spatial average change (Figure 19). By contrast, average precipitation changes have equivalent spread in both cases or only minor reduction in the temperature controlled analysis (Figure 19).

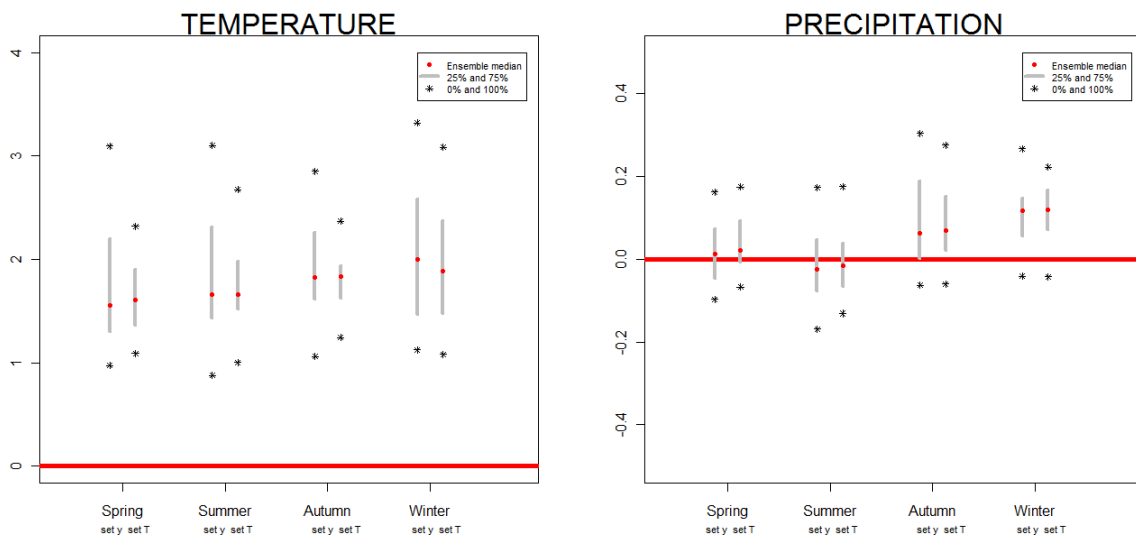
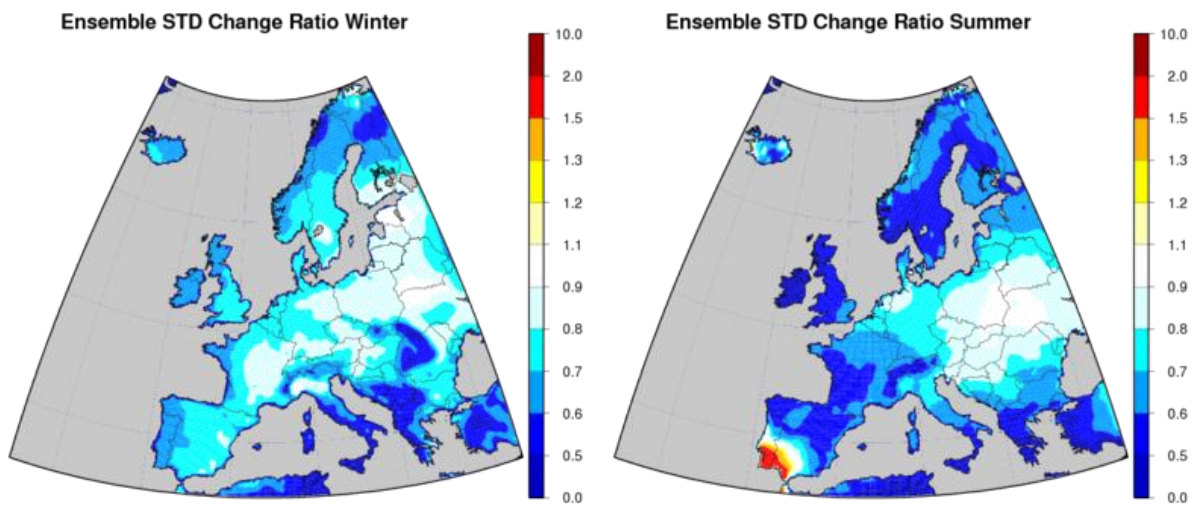


Figure 19: spatial average over land of changes in Temperature (left) and precipitation (right), together with the range of changes for the GCM-RCM ensemble (median, 25-75% range and min and max values). “Set y” refers to fixed time future period (2031-2060), “set T” to the temperature controlled (+2°C) period.

In order to investigate the spatial structure of the spread difference, we show in Figure 20 the distribution of the ratio between the standard deviation for temperature and precipitation as determined in the temperature controlled period versus that in a fixed time period. We remark that

this ratio has lower values near coastal areas and higher values in more continental regions (eg. eastern Europe). This can be tentatively explained by the fact that over oceans, the regional temperature is largely constrained by the global model due to using sea surface temperatures for the GCMs. This means that over oceans and adjacent areas predominantly only the regional anomaly of the GCM at a +2°C global warming contributes to uncertainty in the temperature controlled analysis, while in the fixed time analysis the global sensitivity of the global models contribute in addition. Over continents an additional source for model spread contributes equally in both cases: The full breath of regional feedbacks that the regional models are able to simulate. The net effect is a smaller reduction uncertainty over continental areas, where regional feedbacks are more important. Interestingly, the same effect (larger reduction of uncertainty) is also apparent in mountainous regions like the Alps or the Carpathians. This can be related to a similar mechanism, since upper air temperature is much stronger controlled by the global model than near-surface temperature. For precipitation the ratio remains close to 1 in winter and decreases in summer over Western Europe, especially in areas where a drying change occurs.



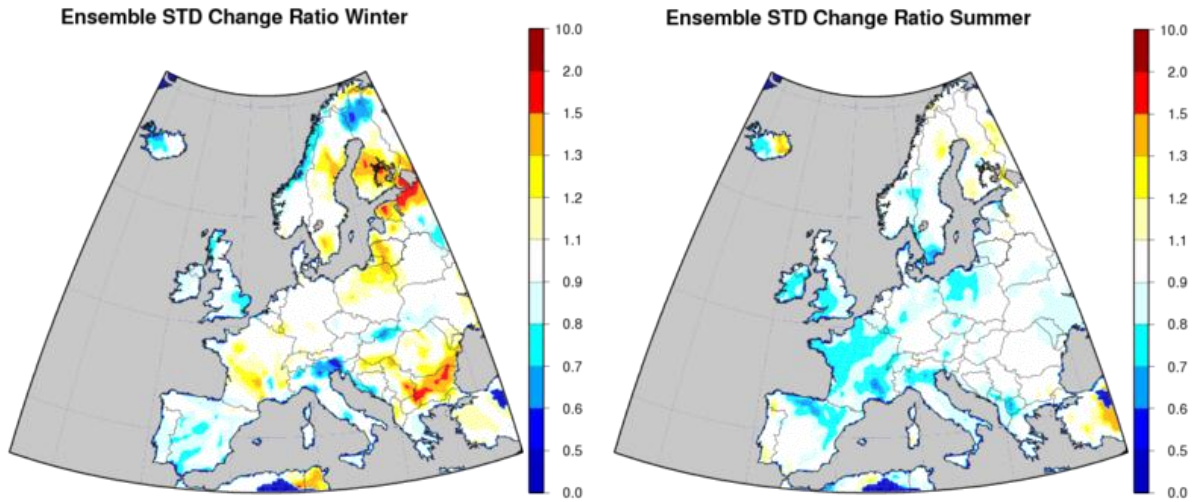


Figure 20: Top: distribution of the ratio of the temperature change standard deviation for the +2°C periods by that obtained for the fixed time period. Bottom: Same as top but for precipitation instead of temperature. Left panels stand for the winter season and right panels for the summer season.

We also present the same ratios for changes in I99 winds and SLP. Figure 21 shows the winter (left) and summer (right) spread ratios for the I99 winds. The + 2C periods indicate a noisy response either by region or by season. Conversely, the SLP spread ratios show coherent decrease in uncertainty across all of Europe in the summer and Western Europe in the winter (figure 21). In +2C case the magnitude of these decreases is around 20-30% in winter (except for the far north, which experiences a large increase in uncertainty) and up to 30-40% in summer.

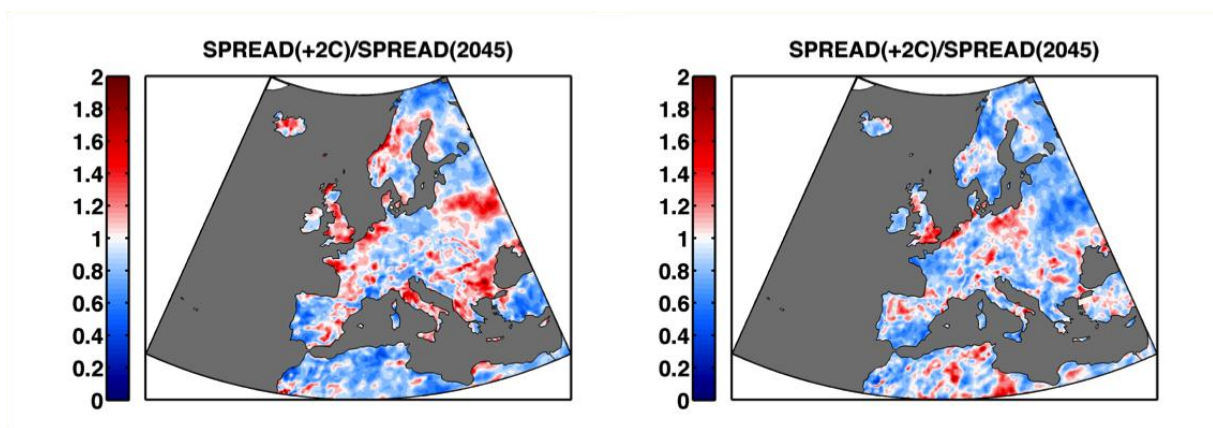


Figure 21 : Winter (left) and Summer (right) Spread ratios of I99 winds during the +2C period versus Time. Blue colors indicate a reduction in uncertainty during the temperature-based periods relative to the time-based period, warm colors the reverse.

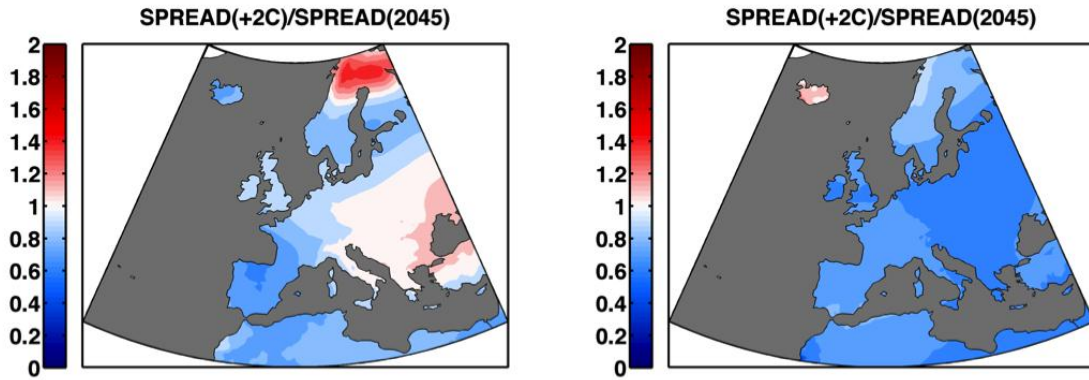


Figure 22: Winter (left) and Summer (right) Spread ratios of SLP during the +2C period versus Time. Blue colors indicate a reduction in uncertainty during the temperature-based periods relative to the time-based period, warm colors the reverse.

Finally we also have briefly investigated the possible influence of bias correction on the estimation of changes, but results are too preliminary to be fully detailed and discussed here.

## Conclusions and perspectives

An analysis of robust patterns of climate change in Europe in the ENSEMBLES A1B regionalized scenario has been carried out for a +2°C global warming compared to preindustrial times. The main results are as follows:

- A global temperature change of +2°C induces an equivalent or slightly weaker warming over coastal areas of North-Western Europe in all seasons, but a more intense warming (up to +3°C) in Northern and Eastern Europe in Winter and in Southern Europe in Summer;
- Under such an assumption, extreme daily maximum temperature follows the same robust trends with an increased amplitude of up to more than 4°C in their 20-year return value; a much larger warming (up to more than 6 degrees) is projected for Scandinavia for extreme cold daily minima in winter while in summer warming of cold daily minima remains limited;
- Precipitation is robustly increasing on average over Central and Northern Europe in winter and only over Northern Europe in summer, while precipitation decreases in Central/Southern Europe in summer; most intense heavy precipitation robustly increase everywhere and in both seasons;
- Such changes in temperature and precipitation also occur assuming a +1.5°C change, with, in general, a linearly scalable amplitude; however in some cases like temperature daily minima over snow covered regions, some nonlinear amplification is found, probably due to snow albedo feedback;
- Extreme winds are found to robustly increase under the +2°C warming assumption in parts of Central Europe in winter, associated with more zonal westerly flows, while in summer wind extremes increase in Northern Europe; no robust extreme wind decrease is predicted;
- Sensible and latent heat flux changes have a strong seasonality with increasing (almost everywhere) evapotranspiration in spring, while it is decreasing in South/Central Europe; sensible heat fluxes have a reverse evolution with an even higher amplitude in South/Central Europe; In summer less clouds in this area allow a more intense net radiation input in this area. However models may overestimate evapotranspiration in spring, leading to an exaggerated drying and sensible heat flux increase in summer;
- The analysis also led us to conclude that a +2°C change is, on average, approximately equivalent to a change for the 2031 – 2060 period in the A1B scenario, with effect of the global temperature sensitivity only important for regional temperature and sea-level pressure but not for other variables;

- While it does not qualitatively affect the robust patterns of climate changes for temperature and precipitation, the bias correction may in some areas slightly modify the amplitude of temperature changes; precipitation changes appear less sensitive to bias correction.

## References

Boberg, F. & J. H. Christensen (2012) Overestimation of Mediterranean summer temperature projections due to model deficiencies. *Nature Climate Change*, 2, 433-436.

Fischer, E. and C. Schär (2010) Consistent geographical patterns of change in high-impact European heat waves. *Nature Climate Change*, 3, 398-403.

Fischer, E. M., J. Rajczak & C. Schär (2012) Changes in European summer temperature variability revisited. *Geophysical Research Letters*, 39.

Haylock M.R., Hofstra N., Klein Tank A.M.G., Klok E.J., Jones P.D., New M. (2008) A European daily high-resolution gridded data set of surface temperature and precipitation for 1950-2006. *Journal of Geophysical Research* 113, D20119

Hewitt, C. D. & D. J. Griggs (2004) Ensembles-based predictions of climate changes and their impacts. *Eos*, 85, 566.

Kjellström, E., Nikulin, G., Hansson, U., Strandberg, G. and Ullerstig, A. 2011. 21st century changes in the European climate: uncertainties derived from an ensemble of regional climate model simulations. *Tellus* **63A**, 24–40.

Nakićenović N., Alcamo J., Davis G., de Vries B., Fenhann J., Gaffin S., Gregory K., Grubler A., Jung T.Y., Kram T., La Rovere E.L., Michaelis L., Mori S., Morita T., Pepper W., Pitcher H., Price L., Keywan R., Roehrl A., Rogner H.-H., Sankovski A., Schlesinger M., Shukla P., Smith S., Swart R., van Rooijen S., Victor N., Dadi Z., 2000, Emission scenarios, A Special Report of Working Group III of the Intergovernmental Panel on Climate Change, Cambridge Univ. Press, New York, N.Y., 599 pp.

Samuelsson, P., Kourzeneva, E. and Mironov, D., 2010: The impact of lakes on the European climate as simulated by a regional climate model. *Boreal Env. Res.* **15**, 113-129.

Stegehuis, A., R. Vautard, P. Ciais, R. Teuling, M. Jung and P. Yiou, 2012: Summer temperatures in Europe and land 1 heat fluxes in observation-based data and regional climate model simulations, *Climate Dynamics*, in press.

Teuling, A. J., M. Hirschi, A. Ohmura, M. Wild, M. Reichstein, P. Ciais, N. Buchmann, C. Ammann, L. Montagnani, A. D. Richardson, G. Wohlfahrt & S. I. Seneviratne (2009) A regional perspective on trends in continental evaporation. *Geophysical Research Letters*, 36.

Thiemeßl, M. J., A. Gobiet, and A. Leuprecht (2011), Empirical-statistical downscaling and error correction of daily precipitation from regional climate models, *Int. J. Climatol.*, 31(10), 1530-1544, doi:10.1002/joc.2168.

Themessl, M. J., A. Gobiet, and G. Heinrich (2012), Empirical-statistical downscaling and error correction of regional climate models and its impact on the climate change signal, *Clim. Change*, 112(2), 449-468, doi:10.1007/s10584-011-0224-4.

Zampieri, M., F. D'Andrea, R. Vautard, P. Ciais, N. de Noblet-Ducoudre & P. Yiou (2009) Hot European Summers and the Role of Soil Moisture in the Propagation of Mediterranean Drought. *Journal of Climate*, 22, 4747-4758.